Thermo-optic durability of cool roof membranes: Effect of shape stabilized phase change material inclusion on building energy

Thermo-optic durability of cool roof membranes: effect of shape stabilized phase change material inclusion on building energy efficiency

C. Fabiani[1], C. Piselli[1,2], A.L. Pisello[1,2]

[1]*CIRIAF - Interuniversity Research Centre, University of Perugia, Italy. Via G. Duranti 63 06125 Perugia (Italy)*

[2]*Department of Engineering University of Perugia, Italy. Via G. Duranti 93 06125 Perugia (Italy)*

Abstract

Cool roofs represent an acknowledged passive cooling technique aimed at reducing the amount of solar radiation absorbed by buildings and producing indoor overheating, particularly, in summer conditions. Cool roofs owe their unique behavior to improved thermo-optic performances which, however, have been shown to deteriorate when exposed to intense atmospheric weathering. In this context, the authors produced a shape stabilized composite with improved heat storage performance, by adding 15, 25 or 35 weight percentage of non-encapsulated phase change materials (PCMs) to the original blend of a liquid waterproof-polyurethane-based cool membrane. The behavior of such composite material, when exposed to accelerated temperature, humidity, and UV radiation cycles by means of standardized long-term weathering tests (QUV test), is investigated. The final aim of the study is to clarify if the PCM inclusion could help the membrane to better behave during the course of the time, because of thermal stress reduction. In order to do so, controlled atmospheric forcing and surface temperature continuous monitoring are used to investigate the degradation of the membrane produced by the imposed weathering stress. Results show that the introduction of 25% PCM in weight optimizes the superficial finishing characteristics of the prototype, allowing to maintain a more stable thermo-optic behavior, reducing both the thermal-induced degradation and the leakage phenomenon.

Keywords: Cool roofs, Phase change material, Shape stabilize material, Weathering analysis, QUV, Thermal energy storage in buildings,

1. Introduction

In the last decades, the awareness about the energy and environmental role of the built environment to meet the European 2020 targets [1] has attracted the focus of researchers [2]. Several solutions for building energy efficiency were developed and acknowledged [3]. In particular, the energy consumption for cooling has been gaining attention due to the raising use of active cooling systems for contrasting the overheating associated to climate change and urban development [4]. Indeed, a worldwide increase of cooling degree days was demonstrated [5]. Therefore, the introduction of passive cooling techniques, capable of reducing summer overheating phenomenon, could play a significant role in the achievement of the global energy consumption reduction targets [6]. Such mitigation and adaptation strategies are effective both at the building scale and at the district or city scale for the restoration of natural passive cooling [7]. Among passive cooling strategies, cool materials are capable to induce a negative radiation forcing by reflecting the shortwave radiation back to space [8]. Therefore, they allow to counteract the global warming, cooling down urban heat islands [9], and reduce the cooling energy use and the associated demand for power, consumption of fuel, greenhouse gas emissions, and air pollutants in buildings [10]. In details, direct energy savings and emission reductions can be achieved thanks to the reduction of envelope solar heat gains [11, 10], while indirect savings from reducing the air temperature difference across the building envelope [12, 13]. In particular, cool roofs were demonstrated to save annual energy consumption in all buildings needing for cooling, with negligible heating penalties in winter, precluding the need to install any air conditioning system under certain boundary conditions [14]. For instance, Herná ndez-Pé rez et al. [15] showed a daily heat gain reduction through the roof up to about 80% thanks to a cool coating with respect to a conventional roof. Moreover, bismuth titanate (BTO) was demonstrated to be a potential cool pigment with even higher reflectance property than the conventional TiO_2 pigment, for energy saving applications [16].

On the other hand, the proper inclusion of phase change materials (PCMs) in the building envelope as passive thermal energy storage application enhances its energy storage capability [17, 18]. Therefore, indoor thermal

conditions are improved by balancing the environmental temperature and dampening its fluctuation [19]. In this view, one of the main technical issues is how to effectively integrate such material within the building envelope [20], while preventing leakage and volatilization and ensuring material conservation [21]. To solve this problem, shape-stabilized PCMs is one of the methodologies currently being used for encapsulation [22]. It consists on the fixation of the phase change material within a matrix, by blending it with a suitable polymer, which results in the suppression of leakage in the liquid phase [23]. Different shape-stabilization procedures were tested for various applications, e.g. a form-stable composite using diatomite (a type of natural non-metallic mineral material) as supporting material [24]. This procedure can be effectively implemented also by coupling cool roof materials and PCMs [25, 26]. The combination of high reflectivity and phase change materials for the building envelope has been narrowly studied, showing potentialities both for building energy efficiency [27] and urban heat island phenomenon mitigation [28]. Lu et al. [29], for example, developed and experimentally monitored a novel roof coupling a PCM-eutectic mixture layer (homogeneous mixture of two materials) and a cool roof coating, which showed a smoother temperature fluctuation and higher thermal insulation with respect to the simple cool roof. Focusing on cool roof coating thermal stress reduction, Saffari et al. [30] defined the optimum PCM melting temperature to reduce cool roof membrane thermal stress, while minimizing building annual energy needs in different climate zones worldwide.

Nevertheless, the demonstrated benefits achievable by such strategies can be compromised during their life span due to material aging associated to weathering [31], soiling [32, 33, 34], and biological growth [35]. Although albedo changes induced by weathering, they can be reduced by an accurate maintenance procedure, e.g. wiping, rinsing, and washing [36]. However, the same technique is not as effective in reducing natural weathering alterations. Additionally, although cool materials aging seems not to represent a barrier for their energy efficiency, performance loss over time must be understood [37]. Several studies quantified the effect of natural exposure on solar reflectance [38, 39]. For instance, Ferrari et al. [40] analyzed the influence of natural aging on the solar reflectance of clay roof tiles.

De Masi et al. [41] found, through in-field test, that the solar reflectance of an acrylic white paint for cool roof applications can decrease from 0.67 to 0.48 after 1 year of exposure to the outdoor environment. Similarly, Aoyama et al. [42] demonstrated the increased durability due to the self-cleaning

capability of a high-reflectance coating subjected to outdoor exposure test. However, such in-field tests require long-time exposure to provide interesting results. Therefore, accelerated weathering techniques, such as QUV test [43], have been developed to provide a shorter test period. In such a test, materials are alternately exposed to temperature cycling, UVA radiation, and water condensation to accelerate natural environments with higher stress, without changing the failure mechanism [44]. The QUV test is typically used to assess materials mechanical failure, but it can also be used to predict the variation in the thermo-optical performance of materials [45]. Since no unequivocal correspondence can be established between accelerated and real weathering due to the large variability on the possible local boundary conditions, real exposure is generally preferred to the accelerated one. However, QUV analysis can produce acceptable information in terms of comparative behavior of the investigated products with a lower effort in terms of experimental time. Santunione et al. [46], for instance, assessed the capability of an accelerated test method to investigate the consequences of biological aggression on coating materials.

To verify the durability of materials thermal-energy performance before and after the aging process, dynamic analysis can be carried out in controlled conditions [47]. This procedure allows to investigate the dynamic behavior of building materials and components with a better reliability than real building applications, frequently affected by extra-variables such as occupancy [48]. Ricciu et al. [49] used this methodology for the thermal characterization of different insulating materials, compared to more traditional procedures, while D'Alessandro et al. used it to characterize the thermal buffer capability of innovative PCM-doped concretes for structural applications [50]. In order to assess the performance of PCM-doped cool roof tiles, Chung and Park [51] simulated summer weather conditions in an artificial environment. The measurements enabled to demonstrate the capability of PCM to further reduce roof external surface temperature, while improving indoor thermal comfort throughout the year.

Based on the above, a novel composite material combining polyurethane liquid waterproof-polyurethane-based cool membrane with different percentages of non-capsulated PCMs was developed for roof applications [52, 26]. When combining PCMs and cool roofs, exposure to sun, rain, and wind are critical factors to be taken into account, since they significantly influence the thermo-mechanical response of the membrane, determining the detrimental leakage phenomenon. Therefore, the composite material was exposed to

accelerated weathering long-term tests (QUV test), to assess the cool membrane vulnerability to real environmental forcing. In a previous paper [45], the same authors evaluated the influence of PCMs inclusion, on the durability of the cool membrane mostly in terms of thermal properties, morphology, and mechanical response. Following up from these studies, the purpose of this work is to further analyze the capability of PCMs to preserve the cool membrane thermal-energy performance over time, due to thermal stress reduction. In detail, thermo-energy dynamic-analysis of the aged composite material was developed in a controlled environmental chamber to assess the role of the PCM in reducing the PCM-doped cool roof surface temperature [48, 50].

2. Materials and sample preparation

In this work, the long-term durability of a polyurethane-based-white-liquid membrane for non-sloped roof applications developed by the authors in a previous research work [52, 26] is experimentally investigated. The aforementioned membrane is optimized by using titanium dioxide (TiO_2, in the form of rutile) and hollow ceramic micro-spheres, to increase its passive cooling potential. Additionally, an organic paraffin with a melting point of 25 °C and a heat storage capacity of 148 $kJ \cdot kg^{-1}$ is also introduced within the mixture, with the aim of preserving better spectral reflectance in the near infrared region of the solar spectrum. Additionally, the smallest possible alteration during the course of accelerated weathering (QUV) tests together with the maintaining of the required flexibility and superficial finishing characteristics, was also sought.

The prototype membranes were produced by simply mixing the solid-state non-encapsulated paraffin within the membrane tank with liquid polyurethane, while keeping an ambient temperature of 20 °C to prevent the PCM from melting during this phase. In the previous works, three different specimens were produced, i.e. a reference "pure-cool" membrane with no additives (noOPT), a cool membrane with "optimized-cool" surface (OPT) and three cool membranes with 15%, 25%, and 35% in weight of PCM added to the original mix design with titanium dioxide and the micro-spheres, i.e. 15PCM, 25PCM and 35PCM, respectively (see Figure 1).

Here, only the optimized-cool and the three PCM-doped membranes were selected to perform a durability investigation of the prototypes against temperature and radiation-induced mechanical stresses. In particular, four square samples with the dimension of 10 cm×10 cm were collected for every considered membrane, and exposed to different accelerated weathering times, i.e. 0, 15, 30 and 60 days.

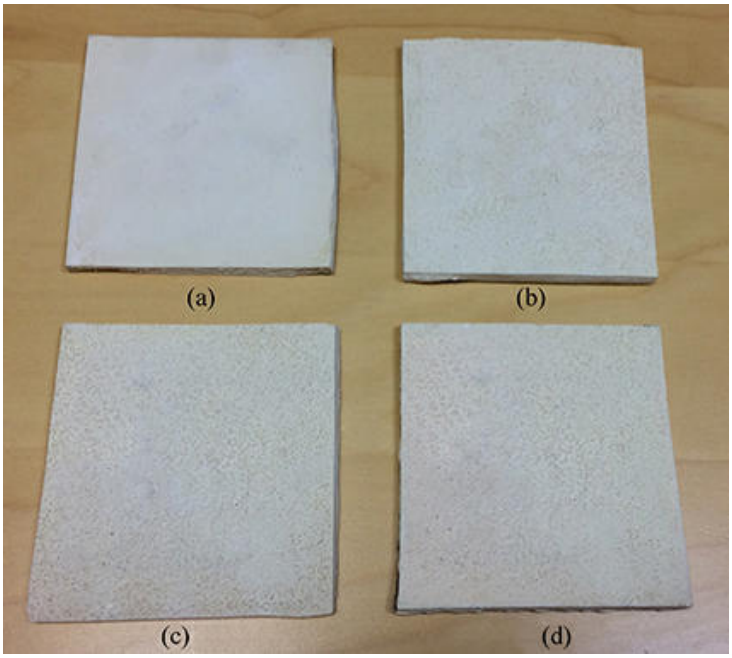

Figure 1: Investigated polyurethane membranes: (a) OPT, (b) 15PCM, (c) 25PCM, and (d) 35PCM, before the accelerated weathering procedure.

3. Experimental methodology

As reported in Figure 2, the research procedure consisted of the following main steps:

- development of the proposed cool roof solution through the integration of an organic PCM, i.e. paraffin-based material, into the polyurethane-based cool membrane in different percentages [52, 26];

- accelerated weathering procedure of the different membranes according to ASTM D 4329-99 (Standard Practice for Fluorescent Ultraviolet

(UV) Lamp Apparatus Exposure of Plastics) [53] and ASTM G154 - 06 (Standard Practice for Operating Fluorescent Light Apparathus for UV Exposure of Nonmetallic Materials) [54];

- surface characterization of the membranes in terms of spectral near normal-hemispherical reflectance according to ASTM E903-12 (Standard Test Method for Solar Absorptance, Reflectance, and Transmittance of Materials Using Integrating Spheres) [55];

- thermal characterization of the membranes at different aging times, i.e. non-aged, 15, 30, and 60 days of aging using the sol-air temperature ($T_{Sol-air}$);

- thermal characterization of the non-aged membranes using a halogen UV-lamp and comparison with the profiles from the sol-air temperature ($T_{Sol-air}$) analysis.

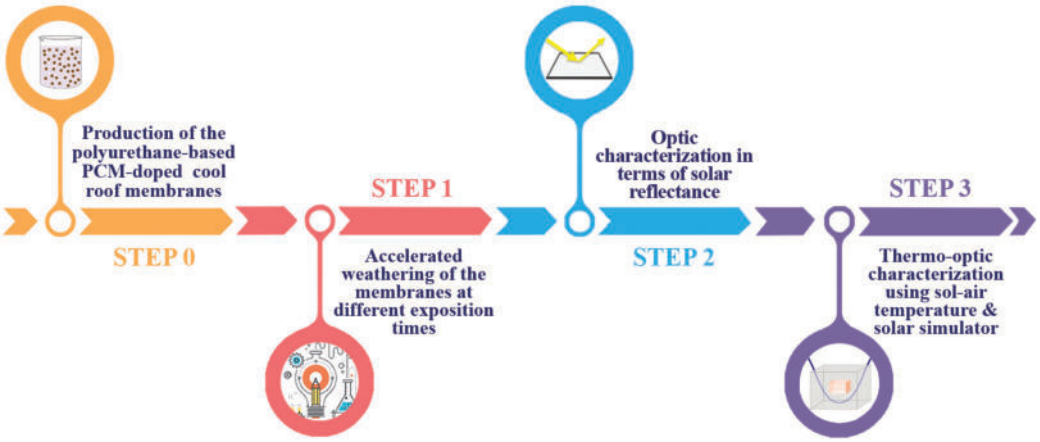

Figure 2: Schematic representation of the main steps carried out in this work

.

3.1. Accelerated weathering test

The accelerated aging test was carried out by usign a QUV machine (QUV Accelerated Weathering Tests, Q-Lab) and according to the international standards ASTM D 4329-99 [53], linked to the operative procedure described in the ASTM G154-06 [54]. The samples were repeatedly exposed to the following forcing conditions:

- 8 hours of UVA radiation (340 nm, energy of 0.77 $W \cdot m^{-2}$) at 50 °C;

- 2 hours in humid condition (100 RH%) at 40 °C;

- 2 hours in humid condition (100 RH%) at 20 °C.

According to ASTM G154-06 standard, any exposure conditions, provided that they are fully described, may be used in the investigation procedure. All this considered, the conditioning cycle used in this work was specifically designed by the authors in order to reproduce environmental conditions that could be representative of the peak temperature and humidity conditions characterizing climate areas where cool roof solutions are typically recommended and applied as passive cooling systems for building energy efficiency.

The effect of the accelerated weathering test on the different samples of cool membranes was evaluated after 15, 30, and 60 days of exposure, based on the common practice derived from the two reference ASTM standards [53, 54]. More in detail, three samples per type were exposed to the test. The first series of samples, one for each type (OPT, 15PCM, 25PCM, and 35PCM), was extracted out of the machine after 15 days, the second series was extracted after 30 days, and the last series was extracted after 60 days.

3.2. Spectral near normal-hemispherical reflectance

The in-lab optical characterization of all the samples was carried out by means of a Solid Spec 3700 UV–vis–NIR spectrophotometer equipped with a 60 mm integrating sphere coated with barium sulfate, in the range 300–2500 nm according to the ASTM E903-12 [55] standard method. Five different spectral near normal-hemispherical reflectance measurements were taken for each of the 16 samples, by measuring different geometrical positions on the membranes, in order to produce a reliable statistic representation of the optic behavior of the innovative coatings.

3.3. Thermal monitoring in real dynamic conditions

The thermal characterization of the membranes was carried in two different stages. First, each membrane was exposed to a hygro-thermal conditioning cycle using the sol-air temperature. Secondly, the non-aged samples were exposed to an additional hygro-thermal forcing procedure, making use of a

solar simulator to reproduce the incoming radiative flux. The former procedure was aimed at evaluating the differential response of the membranes after different aging times; the latter, at comparing the thermal profiles produced using the sol-air temperature (defined in more details in the following) with the ones registered using the solar simulator.

Both analyses were carried out using an ATT DM340SR climatic chamber equipped with a test compartment (601 mm×810mm×694 mm) where it is possible to obtain a temperature- and humidity-controlled environment in the range -40–180 °C± 0.5 °C and 10–98% ±3% of RH [56]. The chamber is also equipped with a solar simulator, i.e. a halogen lamp operating in the power range 600 to 1200 W (solar spectrum shown in Figure 3), and 12 PT-100 temperature sensors. The environmental chamber ensured the high stability of the tests, compared to field experiments, and the repeat ability of the same experiments for bench-marking purposes.

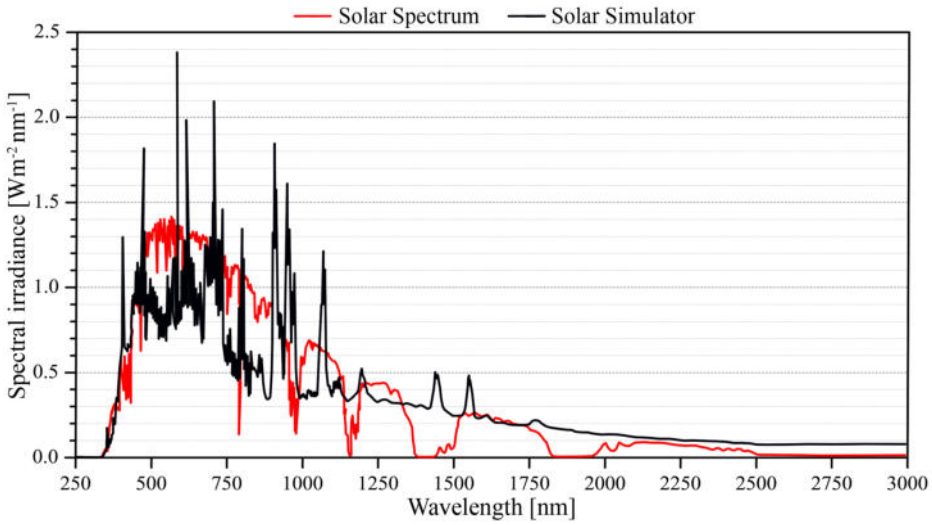

Figure 3: Spectrum of the solar simulator (halogen lamp) compared to the AM 1.5 direct solar spectrum from ASTM G173–03(2012) (Standard Tables for Reference Solar Spectral Irradiances: Direct Normal and Hemispherical on 37° Tilted Surface) [57]).

During the experimental campaign, each type of membrane was housed within the controlled environment of the climatic chamber, and exposed to specifically designed environmental cycles. More in detail, real meteorological data from a weather station located on the rooftop of a University building

located in central Italy (Perugia) were used to investigate the effect of the selected phase change materials on the long-term durability of the advanced cool roof membranes. In particular, weather data from a typical hot summer day, i.e. 2017-07-26, were selected to be reproduced within the simulated environment of the climatic chamber (see Figure 5).

During the experimental campaign, the membranes were placed in a specifically designed polyurethane (PUR) sample holder, assembled in order to completely protect and insulate five surfaces out of six, i.e. the four sides and the bottom surface, while leaving the upper one exposed to the controlled environment of the chamber (see Figure 4).
10 T-type thermocouples were shielded with an aluminum tape and used to monitor the thermal behavior of each sample. In particular, five T-type sensors were attached at the upper surface of the membranes, while the remaining five probes were placed at the bottom surface, as shown in Figure 4. The thermocouples were connected to a data acquisition system model cDAQ-9184 equipped with two NI 9213 Spring slots from National Instruments, and programmed in order to read the sensors every 30 seconds. In this way, it was possible to (i) accurately register the surface thermal profile of the roof membranes and (ii) identify the effect of the PCMs throughout the thickness of the samples during the overall extent of the monitoring process.

3.3.1. Sol-air temperature-based cycles

In the first stage of the thermal analysis, each membrane was exposed to a specifically designed, sol-air temperature-based forcing cycle (Tsol cycle), reproducing the local boundary conditions between 6:00 AM and 9:00 PM Local Standard Time (LST).
The Tsol cycle, makes use of the sol-air temperature ($T_{Sol-air}$) to combine temperature and radiative contributions in one single temperature forcing parameter, to be used in combination with the relative humidity profile.

In this case, a broader time interval (between 5:00 AM and 8:00 PM (LST)), was selected. The sol-air temperature for the horizontal roof stratigraphy exposed to the selected weather conditions was computed according to Equation 1 [58]:

$$T_{\mathrm{Sol-air}} = T_{\mathrm{air}} + \alpha I_{\mathrm{g}} R_{\mathrm{se}} - \Delta Q_{\mathrm{ir}} R_{\mathrm{se}} \quad (1)$$

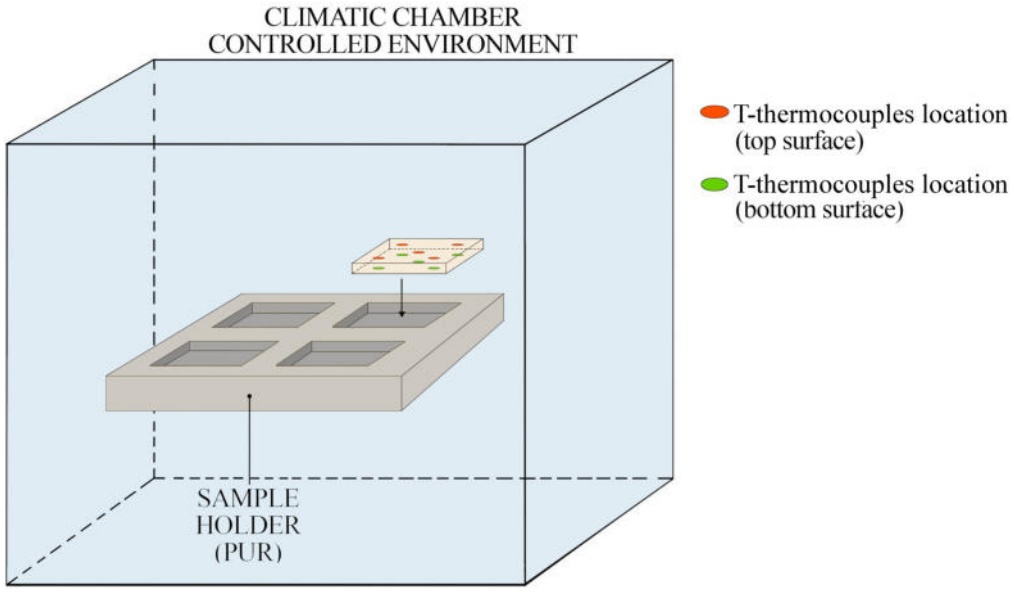

Figure 4: Schematic representation of the experimental setup.

where T_{air} is the outdoor air temperature from the weather file (°C); α is the solar absorptance of the specific membranes; I_{g} is the global solar radiation from the weather file ($\text{W}\cdot\text{m}^{-2}$); R_{se} is the external surface resistance ($\text{m}^2\cdot(\text{K}\cdot\text{W})^{-1}$); and $\Delta\text{Q}_{\text{ir}}$ is the correction to infrared radiation transfer between surface and environment if sky temperature is different from T_{air}, ($\text{W}\cdot\text{m}^{-2}$).

The term R_{se} Equation 1, was set to 0.04 ($\text{m}^2\cdot\text{K}^{-1}\cdot\text{W}^{-1}$), in accordance to the recommendations of ISO 6946:2017 (Building components and building elements – Thermal resistance and thermal transmittance – Calculation methods) [59]. As for the infrared radiation transfer correction, since the roof membrane respresents a upward-facing surface in real applications, $\Delta\text{Q}_{\text{ir}}\text{R}_{\text{se}}$ was imposed to its maximum value, i.e. 3.9 °C [60].

Given that the sol-air temperature depends on solar absorptance, which differs by material, each membrane was separately analyzed and exposed to a unique temperature profile based on its solar absorptance. All the membranes were assumed to be opaque surfaces, therefore, the specific solar absorptance of each surface was calculated as $\alpha = 1 - \rho$, making use of the reflectance

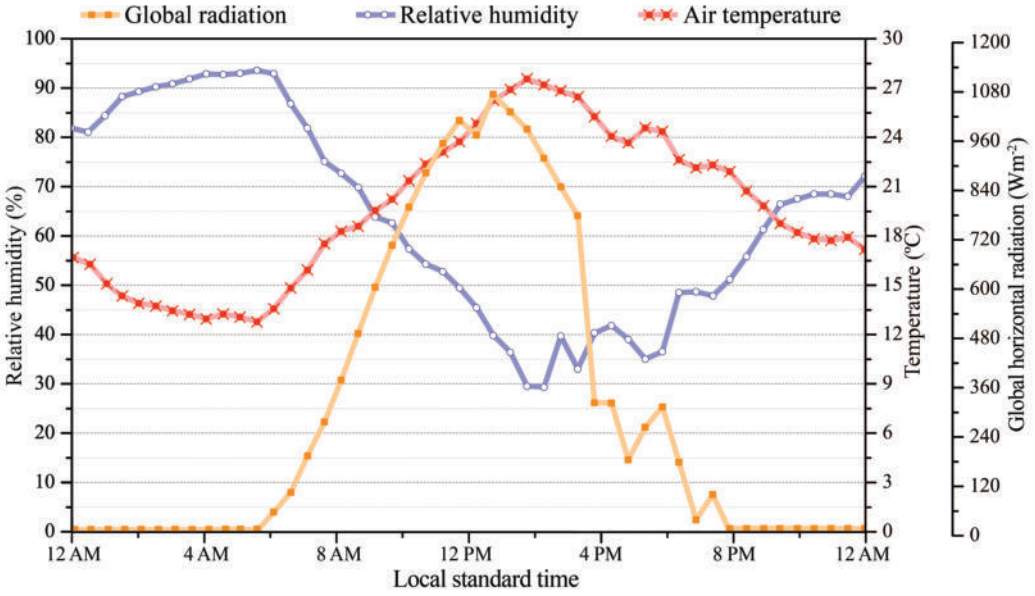

Figure 5: Relative humidity, air temperature, and global radiation (in the range 300 – 2800 nm) values registered by the weather station at Perugia University on July 26, 2017.

values presented in Section 4.1.

3.3.2. Radiation-based cycles

At a later stage, the non-aged membranes were exposed to an additional environmental cycle (the air temperature-radiation based – TaRAD – cycle), which was designed to exactly reproduce the local climatic conditions in terms of outdoor air temperature, relative humidity, and global radiation flux on the horizontal surface from 7:30 AM to 5:30 PM (LST). This specific time range was selected due to technical limitations: the solar simulator only allows to reproduce radiative fluxes above 250 $W \cdot m^{-2}$.

In contrast to the sol-air temperature-based thermal analysis, the investigation procedure carried out using air temperature and radiative flux as two separate boundary conditions allows to simultaneously analyze the thermal behavior of each type of membrane. In this case the surface interaction between the incoming radiation and the material is a real physical phenomenon occurring during the simulation. Therefore, every membrane behaves in a different way, based on its own thermo-optic properties, although exposed to the same conditioning cycle.

All this considered, using solar simulators could significantly reduce experimental time. However, solar simulator are often associated to non-negligible deviations in terms of short-wave radiation accuracy, and lack of long-wave radiative exchange with the sky. In this view, the main purpose of this analysis is to compare the thermal profiles produced using sol-air temperatures with the ones registered using the solar simulator and evaluate the actual deviation between these conditioning techniques.

4. Results and discussions

4.1. Thermo-optic performance of the roof membranes

Results from the solar reflectance measurements as a function of the aging procedure are plotted in Figure 6. As can be seen, at time zero, the non-aged optimized membrane (OPT sample) presents the highest solar reflectance. Despite this, as demonstrated in a previous contribution from the same authors [26], the introduction of the PCMs does not result in chemical variations of the original polyurethane-based substrate. On the contrary, the two components maintain their properties and coexist in a stable form, preserving and globally combining their unique behavior. As a consequence, the external finishing of the membrane is really constituted by the only polyurethane matrix, at least, until the PCM finally leaks out of it reaching the surface. The introduction of the latent doping agent, however, increases the composite surface roughness, due to the presence of PCM agglomerations right beneath the surface.
As a consequence, larger shadows are produced and lower reflectances are obtained with increasing PCM percentages [61]. Said reduction is particularly large in the case of the 35PCM sample, which reaches a reflectance of 0.51, before aging.

By focusing on the long-term performance of the investigated membranes, and assuming a good correlation between accelerated weathering and natural exposition effect, a different resilience capability can be observed. The QUV aging test seriously affects the optimized membrane, which significantly reduces its reflectance with increasing weathering times (according to a quite reasonable linear trend). As for the 15PCM sample, namely the one with the minimum PCM addition, Figure 6 shows a much less stable trend, characterized by an abrupt reflectance decrease after 15 days of aging, while after 30

and 60 days, similar performance compared to the pure membrane are found. Globally, the introduction of the PCM reduces the slope of the linear fitting curve connecting the reflectance measurements at different aging times. This brings the 15PCM sample to obtain a comparable reflectance with respect to the optimized membrane after 60 days aging.

Concerning the 25% PCM-doped solution, this particular PCM concentration shows the most promising long-term performance. The slope of the 25PCM fitting line, indeed, tends to zero in this case.

As for the 35% PCM-doped solution, the highest reflectance reduction is observed in the long-term weathering. As shown in Figure 6, the 35PCM sample solar reflection capability is initially increased, and only finally drops to 0.47 (after 60 days aging).

Furthermore, it should be stressed that both the 25PCM and the 35PCM sample experience an initial reflectance increase. This is probably caused by a positive superficial smoothing, produced by the QUV forcing cycles that reduces the drop shadows effect.

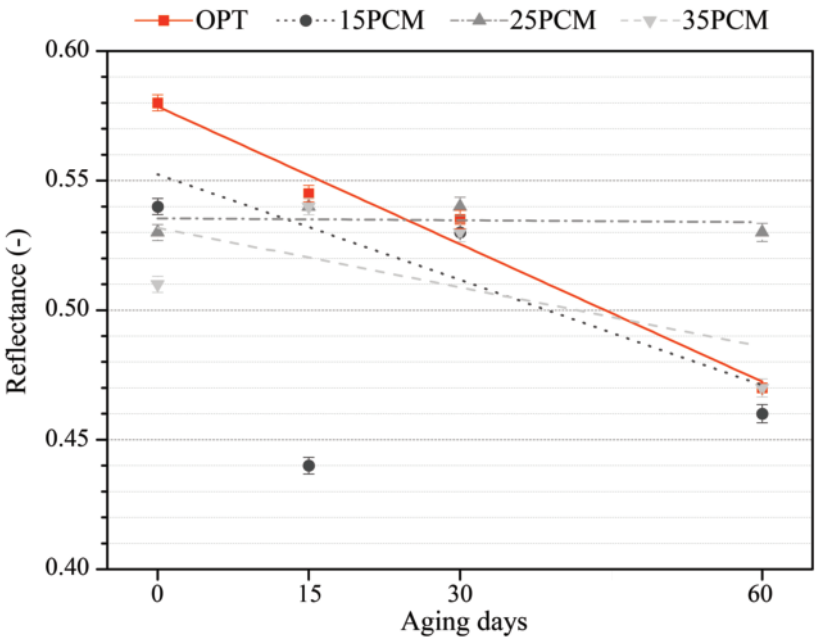

Figure 6: Total solar reflectance for the investigated polyurethane membranes, i.e. OPT-CM, 15PCM-CM, 25PCM-CM, and 35PCM-CM, before and after the accelerated weathering procedure.

Based on the above, we can state that each membrane is differently affected by the QUV test. Figure 7 shows the typical forcing profiles for a single aging day. As can be seen, during the weathering procedure each sample experiences abrupt variations in terms of temperature, relative humidity, and UVA radiation. Such variations produce intense temperature gradients and, consequently, the development of non-negligible stresses and strains in the polyurethane substrate, resulting in a complex micro-cracking pattern that globally concurs to reduce the reflectance of the OPT sample.

The introduction of PCMs, being capable to store part of the heat in the latent form, is expected to reduce such temperature gradients and the albedo degradation with it. However, only the 25PCM sample maintains a higher reflectance throughout the aging. This suggests that PCM concentrations around 15% and 35% do not allow the latent additive to fulfill its buffer task. In particular, it seems that lower PCM concentrations do not guarantee enough energy density to overcome the detrimental mechanical deterioration of the substrate, which consequently experiences a similar thermally-driven micro-cracking process. Therefore, as experienced by a direct visual and tactile inspection, the liquid PCM leaks out of the membrane already after 15 days aging, reducing its surface reflectance.
Higher concentrations, on the other hand, initially allow to produce the expected buffering effect. However, on the long-term the 35PCM sample experiences a similar drop in reflectance to the one found in the 15PCM after 15 days. This, together with the results from the visual and tactile inspection, suggests that leakage eventually occurs also in this case, but only at a later stage and most probably because of the higher PCM concentrations in the composite.

As a consequence, in the long-term, despite the occurrence of different deterioration mechanisms, both the 15PCM and the 35PCM, mostly behave as the OPT membrane.

4.2. Effect of phase change materials on the surface temperature of the aged cool roof membranes

Figure 8 shows the comparison among different surface temperature profiles monitored during the imposed Tsol cycles for each kind of membrane and weathering time. In particular, profiles with the same QUV exposure time are grouped and plotted on the same panel, allowing us to compare

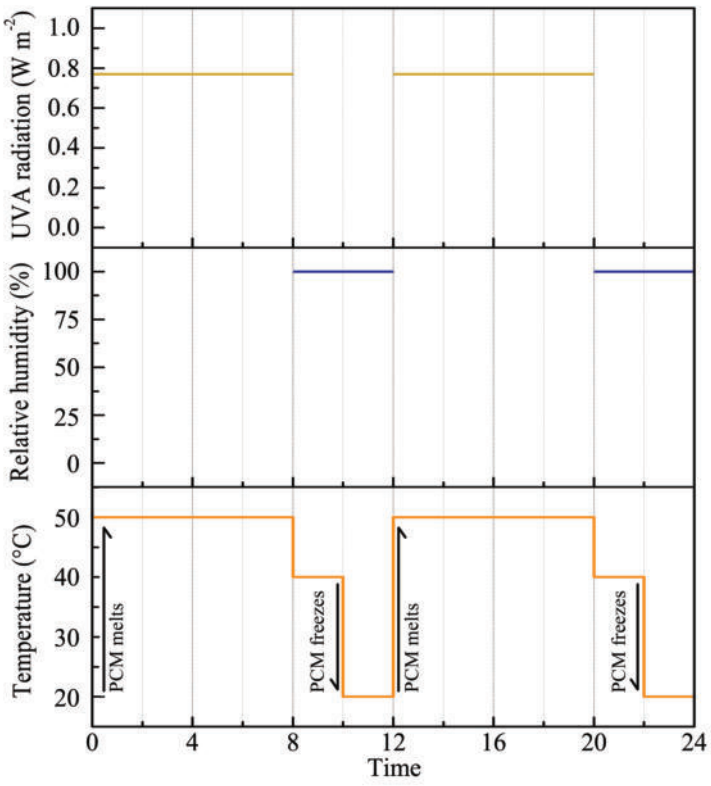

Figure 7: Forcing profiles for a typical QUV aging day.

the differential thermal response of the membranes when exposed to similar weathering conditions.

As expected, at time zero the TiO_2-optimized membrane with no PCM addition produces the lowest surface temperature profile, exceeding 40 °C only in the central part of the day (between 11:45 AM and 1:27 PM (LST), as shown in Figure 10 and Table 1). Concerning the three considered PCM-doped solutions, according to the previously described solar reflectances, an increased temperature trend is produced when increasing the weight percentage of the latent additive in the roofing membrane. However, no significant difference can be seen between the 25 and the 35% PCM solution. After 15 days of accelerated weathering, the reference optimized membrane with no PCM suffers by a non-negligible temperature increase, featuring a wider temperature bell with a peak value of 45.3 °C versus the 41.2 °C registered before the aging process. Additionally, Figure 10 shows that the 15-days-aged op-

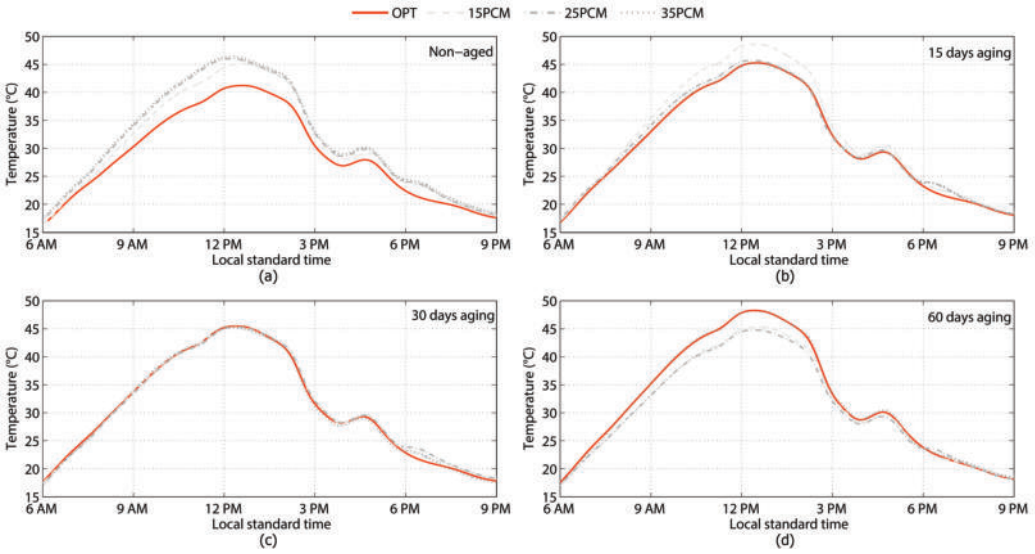

Figure 8: Comparison among the different superficial temperature profiles from the Tsol cycles considering the same accelerated weathering time, i.e. (a) 0 days, (b) 15 days, (c) 30 days, (d) 60 days.

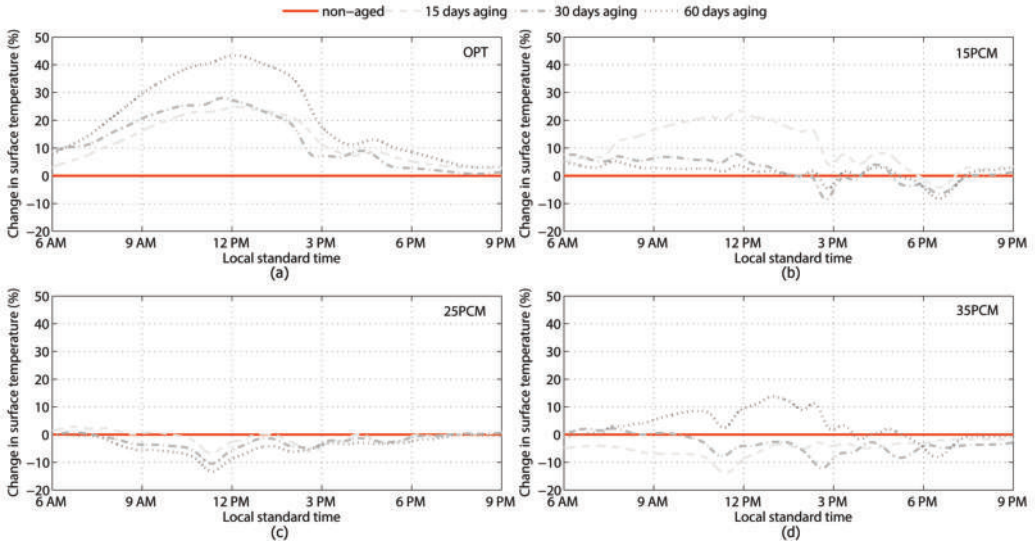

Figure 9: Change in surface temperature of the considered membranes, i.e. (a) OPT, (b) 15PCM, (c) 25PCM, (d) 35PCM, when exposed to 15, 30, and 60 days of accelerated weathering procedure with respect to the maximum air temperature difference registered in the selected day $(T_{aged} - T_{non-aged}) / (T_{air,max} - T_{air,min})$.

Table 1: Peak temperature value and local standard time at which it was registered in each of the selected membranes, considering different aging periods (0, 15, 30, and 60 days).

Aging	opt		15PCM		25PCM		35PCM	
days	LST	T	LST	T	LST	T	LST	T
	[hh:mm]	[°C]	[hh:mm]	[°C]	[hh:mm]	[°C]	[hh:mm]	[°C]
0	12:52	41.2	12:27	45.1	12:11	46.0	12:11	46.4
15	12:24	45.3	12:31	48.6	12:13	45.7	12:15	45.2
30	12:38	45.5	12:26	45.7	12:24	45.7	12:10	45.7
60	12:25	48.3	12:31	45.3	12:23	45.3	12:28	48.1

timized membrane maintains its temperature above 40 °C for about 3 hours and 52 minutes, while the original material only exceeded this limit for 1 hour and 45 minutes. Such an abrupt variation of the optimized membrane performance, allows both the 25PCM and the 35PCM sample to obtain similar thermal performance compared to the OPT sample after 15-days-aging. The 15PCM sample, on the other hand, similarly to the optimized membrane experiences a significant surface temperature increase producing a temperature peak of 48.6 °C.
After 30 days, all the membranes seem to behave in a similar way and are associated to an almost indistinguishable trend. Finally, after 60-days-aging, the reference membrane with no PCM and the 35PCM solution show the worst thermal response reaching more than 48 °C in the central part of the day.

Based on the aforementioned results, we can state that the addition of PCM to the original polyurethane mixture affects the stability of the membranes thermo-optical performance in time. In order to more carefully investigate this phenomenon, we focused our attention on the percentage change in surface temperature, defined as the difference between the surface temperature of the aged sample (T_{aged}) and the corresponding non-aged one ($T_{non-aged}$), over the maximum air temperature difference registered in the selected day ($T_{air,max}$–$T_{air,min}$). Figure 9 depicts said variation, grouping the membranes in four different panels (one for each type of membrane), i.e. OPT, 15PCM, 25PCM, and 35PCM.
Results demonstrate that the optimized membrane with no PCM addition is associated to the highest variations. In more detail, after 15 days of aging, an average variation by 10.2% is found, while average differences by about

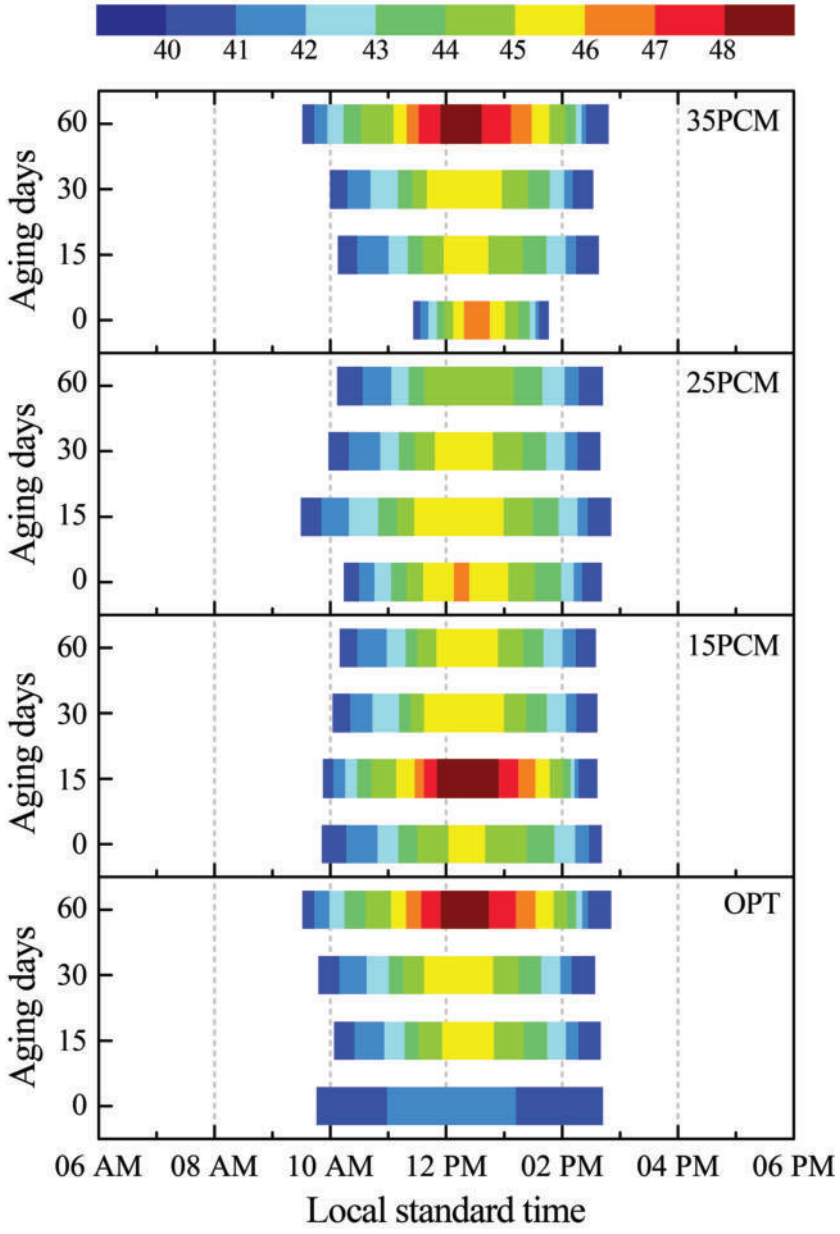

Figure 10: Time spent at temperatures above 40 °C for the investigated polyurethane membranes, i.e. (a) OPT-CM, (b) 15PCM-CM, (c) 25PCM-CM, and (d) 35PCM-CM, before the accelerated weathering procedure.

10.9 and 17.6% characterize the membrane after 30 and 60 days of weathering, respectively. Globally, the weathering process causes an abrupt decrease in the thermo-optic performance of the OPT membrane, which seemed to stabilize in the medium distance and eventually decrease again after 60 days of aging.

Concerning the PCM-doped membranes, all of them maintain a more stable profile in time. However some variations can be detected among the different types considered in this work. In particular, the use of 25%-in-weight of PCM in the selected waterproof application seems to guarantee an acceptable trade-off between reduced deterioration due to thermal expansion and leakage-induced soiling upon weathering. The 25PCM is, indeed, the only application that allows to obtain a negative average temperature change in all three aging conditions (-0.63, -1.99, and -3.11% after 15, 30, and 60 days, respectively). This particular result suggests that the addition of the selected amount of PCM could represent a further optimization of the innovative cool roof membrane, aimed at improving its long-term durability performance.

4.3. Comparison between sol-air temperature and radiation-based forcing

Figure 10 shows the comparison among the surface temperature profiles of the four considered membranes exposed to the TaRAD and the Tsol cycles. As can be seen, the dark-grey-dashed profile, depicting the surface temperature generated by the radiation-based temperature forcing, very well reproduces the shape of the solid red-line trend, representing the thermal behavior of the same membrane exposed to the sol-air temperature-based forcing cycle. However, every graph in Figure 10 shows an average deviation of about 2 °C between the profile produced by the radiation-based temperature forcing (associated to higher temperatures) and the one from the Tsol cycle (the one that uses the sol air temperature simplification). Said difference exceeds the expected experimental error derived from the combination of the acquisition and the environmental forcing system of about 1 °C, and it is probably due to an underestimation of the long-wave radiative exchange with the local environment.

Based on this evidence, a specifically designed correction factor could be introduced to take into account the non-negligible effect of the long-wave exchange, at least when horizontal applications are considered. In any case, the radiation-based forcing allowed to reproduce the thermal response of

the investigated waterproof-polyurethane-based roofing solutions in a rapid and effective way by exposing all the membranes to the same forcing cycle. The interaction between the short-wave incoming solar radiation and the different surfaces is, in this case, a real physical phenomenon that depends on the specific solar reflectance capability of the investigated membranes.

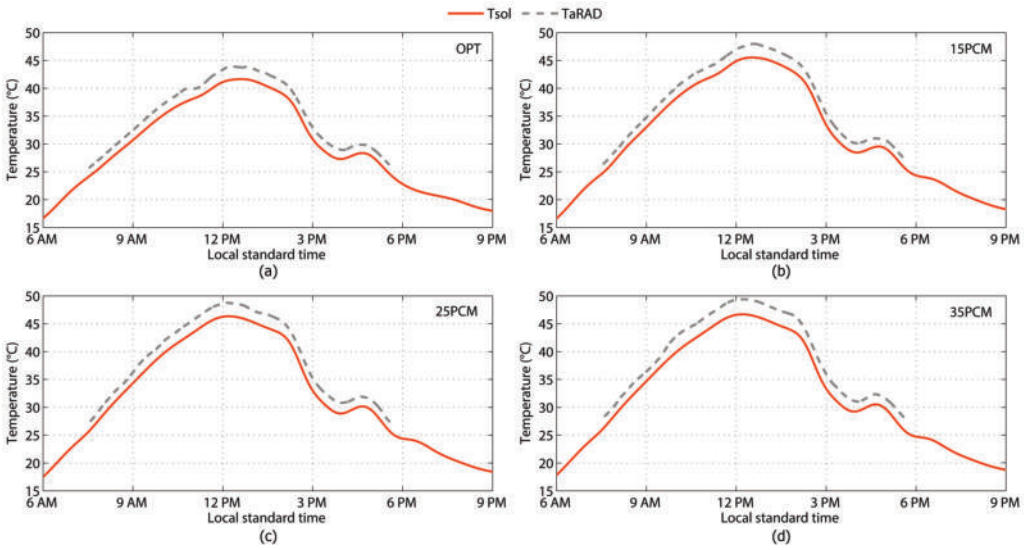

Figure 11: Comparison between the thermal profiles from the TaRAD and the Tsol cycle for the investigated polyurethane membranes, i.e. (a) OPT-CM, (b) 15PCM-CM, (c) 25PCM-CM, and (d) 35PCM-CM, before the accelerated weathering procedure.

5. Conclusions

Building upon previews research aimed at developing an innovative polyurethane membrane including up to 35%-in-weight of phase change materials with a melting temperature of 25 °C, this work tackles the thermo-optic durability of such unique application coupling cool and latent solutions into a composite roofing material for passive cooling purpose.
In more detail, the role of PCMs in improving the cool roof membrane durability when exposed to typical massive thermal fluctuations due to extreme air temperatures and intense radiation from the sun, was assessed.

By shifting from a purely sensible to a partly latent heat storage application, this research aimed to reduce the long-term deterioration of the

membrane due to extreme thermal stresses. In this view, three different roof membranes including organic paraffin in a shape-stabilized solution were developed considering 15%, 25%, and 35% of PCM with respect to the weight of the liquid membrane. Additionally, an optimized cool roof membrane including titanium dioxide was also produced for comparison purpose. Said membranes were later exposed to an accelerated weathering procedure (QUV) for 15, 30, and 60 days, according to ASTM D 4329-99 and ASTM G 154-06, and their optic performance was evaluated in terms of reflection coefficient based on ASTM E903-12 before and after the aging procedure. Finally, the thermal performance of all the samples was investigated and compared in terms of roof surface temperature using controlled environmental forcing. In more detail, an ATT DM340SR climatic chamber equipped with a solar simulator (halogen lamp) was used to reproduce the local boundary conditions of a typical summer day and expose the samples to a fully controlled and reproducible environmental forcing. The behavior of the membranes was compared using sol-air temperature-based forcing cycles, while the potential use of radiation-based conditioning was assessed and bench-marked to the previous methodology.

Results showed that the introduction of the latent additive allows to preserve a more stable solar reflectance capability even after 60 days of aging, particularly when 25% in weight of PCM was added to the original polyurethane-based mixture. Concerning the surface temperature monitoring during controlled environmental forcing, PCM addition to the basic mixture involved lower thermal performance at time zero, but in the meantime, allowed to maintain a more stable behavior with increasing the weathering time. In particular, the detrimental temperature increase registered between the new and the 15-days-aged OPT sample was significantly reduced by the introduction of the PCM. Additionally, the 25% PCM solution not only maintained its thermo-optic performance, but it actually improved, although slightly, after 30 and 60 days of aging. As for the radiation-based conditioning, it was shown that though this methodology tends to overstate surface overheating due to the exclusion of the long-wave radiative exchange with the sky, a specifically designed correction factor could be used to rapidly produce reliable temperature profiles.

In conclusion, the proposed analysis showed how thermal energy storage techniques could be used to improve the thermo-optic durability of water-

proof membranes for roofing applications, frequently exposed to severe degradation due to extreme environmental boundary conditions. In particular, the addition of the proper amount of latent storage material could produce a finishing material capable of improving rather then reducing its passive cooling capability after extreme weathering conditions.

Acknowledgment

Acknowledgment

This research has received funding from the European Union's Horizon 2020 research and innovation program under grant agreement n° 657466 (INPATH-TES). The authors would like to thank Fondazione cassa di Risparmio di Perugia for supporting the investigation about bio-materials within the project SOS CITTÁ 2018.0499.026 and Gabriele Franceschetti and CVR s.r.l. company for assisting the development of cool membranes prototypes with integrated PCMs. Cristina Pisellis acknowledgments are due to "Umbria A.R.CO." project of Regione Umbria for supporting her research within the framework of "SMEET-WELL: SMart building managEment for Energy saving meets WELLbeing" project.

References

[1] L. Saikku, A. Rautiainen, P. E. Kauppi, The sustainability challenge of meeting carbon dioxide targets in Europe by 2020, Energy Policy 36 (2) (2008) 730–742. doi:10.1016/j.enpol.2007.10.007.

[2] N. Soares, J. Bastos, L. Dias Pereira, A. Soares, A. R. Amaral, E. Asadi, F. Lamas, E. Rodrigues, H. Monteiro, M. Lopes, A. Gaspar, A review on current advances in the energy and environmental performance of buildings towards a more sustainable built environment, Renewable and Sustainable Energy Reviews 77 (2017) 845–860. doi:10.1016/j.rser.2017.04.027.

[3] M. Walls, Energy efficiency: Building labels lead to savings, Nature Energy 1 (2017) 17055. doi:10.1038/nenergy.2017.55.

[4] F. Ascione, Energy conservation and renewable technologies for buildings to face the impact of the climate change and minimize the use of cooling, Solar Energy 154. doi:10.1016/j.solener.2017.01.022.

[5] D. Jacob, L. Kotova, C. Teichmann, S. Sobolowski, R. Vautard, C. Donnelly, A. Koutroulis, M. Grillakis, I. Tsanis, A. Damm, A. Sakalli, M. van Vliet, Climate impacts in Europe under +1.5°C global warming, Earth's Futuredoi:10.1002/2017EF000710.

[6] M. Santamouris, Cooling the buildings past, present and future, Energy and Buildings 128. doi:10.1016/j.enbuild.2016.07.034.

[7] M. Kaboré, E. Bozonnet, P. Salagnac, M. Abadie, Indexes for passive building design in urban context–indoor and outdoor cooling potentials, Energy and Buildings 173 (2018) 315–325. doi:10.1016/j.enbuild.2018.05.043.

[8] H. Akbari, H. D. Matthews, Global cooling updates: Reflective roofs and pavements, Energy and Buildings 55 (2012) 26. doi:10.1016/j.enbuild.2012.02.055.

[9] H. Akbari, C. Cartalis, D. Kolokotsa, A. Muscio, A. L. Pisello, F. Rossi, M. Santamouris, A. Synnefa, N. Wong, M. Zinzi, Local climate change and urban heat island mitigation techniques - the state of the art, Journal of Civil Engineering and Management 22 (2016) 1–16. doi:10.3846/13923730.2015.1111934.

[10] P. Rosado, R. Levinson, Potential benefits of cool walls on residential and commercial buildings across california and the united states: Conserving energy, saving money, and reducing emission of greenhouse gases and air pollutants, Energy and Buildings 199. doi:10.1016/j.enbuild.2019.02.028.

[11] T. Xu, J. Sathaye, H. Akbari, V. Garg, S. Tetali, Quantifying the direct benefits of cool roofs in an urban setting: Reduced cooling energy use and lowered greenhouse gas emissions, Building and Environment 48 (2012) 1–6. doi:10.1016/j.buildenv.2011.08.011.

[12] A. H. Rosenfeld, H. Akbari, J. J. Romm, M. Pomerantz, Cool communities: strategies for heat island mitigation and smog reduction, Energy and buildings 28 (1) (1998) 51–62. doi:10.1016/S0378-7788(97)00063-7.

[13] M. Pomerantz, Are cooler surfaces a cost-effect mitigation of urban heat islands?, Urban Climate 24 (2018) 393 – 397. doi:10.1016/j.uclim.2017.04.009.

[14] C. Piselli, M. Saffari, A. de Gracia, A. L. Pisello, F. Cotana, L. F. Cabeza, Optimization of roof solar reflectance under different climate conditions, occupancy, building configuration and energy systems, Energy and Buildings 151 (2017) 81–97. doi:10.1016/j.enbuild.2017.06.045.

[15] I. Hernández-Pérez, J. Xamán, E. V. Macías-Melo, K. M. Aguilar-Castro, I. Zavala-Guillén, I. Hernández-López, E. Simá, Experimental thermal evaluation of building roofs with conventional and reflective coatings, Energy and Buildings 158 (2018) 569–579. doi:10.1016/j.enbuild.2017.09.085.

[16] P. Meenakshi, M. Selvaraj, Bismuth titanate as an infrared reflective pigment for cool roof coating, Solar Energy Materials and Solar Cells 174 (2018) 530–537. doi:10.1016/j.solmat.2017.09.048.

[17] A. de Gracia, L. F. Cabeza, Phase change materials and thermal energy storage for buildings, Energy and Buildings 88. doi:10.1016/j.enbuild.2015.06.007.

[18] M. Song, F. Niu, N. Mao, Y. Hu, S. Deng, Review on building energy performance improvement using phase change materials, Energy and Buildings 158 (2018) 776–793. doi:10.1016/j.enbuild.2017.10.066.

[19] K. Kant, A. Shukla, A. Sharma, Advancement in phase change materials for thermal energy storage applications, Solar Energy Materials and Solar Cells 172 (2017) 82–92. doi:10.1016/j.solmat.2017.07.023.

[20] L. Calabrese, E. Proverbio, A. Frazzica, V. Brancato, F. Grungo, D. La Rosa, V. Palomba, Thermal performance of hybrid cement mortar-PCMs for warm climates application, Solar Energy Materials and Solar Cells 193 (2019) 270–280. doi:10.1016/j.solmat.2019.01.022.

[21] H. B. Kim, M. Mae, Y. Choi, T. Kiyota, Experimental analysis of thermal performance in buildings with shape-stabilized phase change materials, Energy and Buildings 152 (2017) 524–533. doi:10.1016/j.enbuild.2017.07.076.

[22] M. Genc, Z. Genc, Microencapsulated myristic acidfly ash with tio2 shell as a novel phase change material for building application, Journal of Thermal Analysis and Calorimetry 131 (2017) 1–8. doi:10.1007/s10973-017-6781-7.

[23] I. Krupa, P. Sobolčiak, H. Abdelrazeq, M. Ouederni, M. A. Al-Maadeed, Natural aging of shape stabilized phase change materials based on paraffin wax, Polymer testing 63 (2017) 567–572. doi:10.1016/j.polymertesting.2017.09.027.

[24] Z. Rao, G. Zhang, T. Xu, K. Hong, Experimental study on a novel form-stable phase change materials based on diatomite for solar energy storage, Solar Energy Materials and Solar Cells 182 (2018) 52–60. doi:10.1016/j.solmat.2018.03.016.

[25] S. G. Yoon, Y. K. Yang, T. W. Kim, M. H. Chung, J. C. Park, Thermal performance test of a phase-change-material cool roof system by a scaled model, Advances in Civil Engineering 2018. doi:10.1155/2018/2646103.

[26] A. Pisello, E. Fortunati, S. Mattioli, L. F. Cabeza, C. Barreneche, J. Kenny, F. Cotana, Innovative cool roofing membrane with integrated phase change materials: Experimental characterization of morphological, thermal and optic-energy behavior, Energy and Buildings 112 (2016) 40–48. doi:10.1016/j.enbuild.2015.11.061.

[27] P. Lassandro, S. Di Turi, Energy efficiency and resilience against increasing temperatures in summer: The use of pcm and cool materials in buildings, International Journal of Heat and Technology 35 (2017) S307–S315. doi:10.18280/ijht.35Sp0142.

[28] Y. K. Yang, I. S. Kang, M. H. Chung, S. Kim, J. C. Park, Effect of pcm cool roof system on the reduction in urban heat island phenomenon, Building and Environment 122 (2017) 411 – 421. doi:10.1016/j.buildenv.2017.06.015.

[29] S. Lu, Y. Chen, S. Liu, X. Kong, Experimental research on a novel energy efficiency roof coupled with pcm and cool materials, Energy and Buildings 127. doi:10.1016/j.enbuild.2016.05.080.

[30] M. Saffari, C. Piselli, A. de Gracia, A. L. Pisello, F. Cotana, L. F. Cabeza, Thermal stress reduction in cool roof membranes using phase change materials (pcm), Energy and Buildings 158 (2018) 1097–1105. doi:10.1016/j.enbuild.2017.10.068.

[31] S. Tsoka, T. Theodosiou, K. Tsikaloudaki, F. Flourentzou, Modeling the performance of cool pavements and the effect of their aging on outdoor surface and air temperatures, Sustainable Cities and Society 42. doi:10.1016/j.scs.2018.07.016.

[32] M. Sleiman, G. Ban-Weiss, H. E. Gilbert, D. François, P. Berdahl, T. W. Kirchstetter, H. Destaillats, R. Levinson, Soiling of building envelope surfaces and its effect on solar reflectancepart i: Analysis of roofing product databases, Solar Energy Materials and Solar Cells 95 (12) (2011) 3385–3399. doi:10.1016/j.solmat.2011.08.002.

[33] M. Sleiman, T. W. Kirchstetter, P. Berdahl, H. E. Gilbert, S. Quelen, L. Marlot, C. V. Preble, S. Chen, A. Montalbano, O. Rosseler, et al., Soiling of building envelope surfaces and its effect on solar reflectance–part ii: Development of an accelerated aging method for roofing materials, Solar Energy Materials and Solar Cells 122 (2014) 271–281. doi:10.1016/j.solmat.2013.11.028.

[34] M. Sleiman, S. Chen, H. E. Gilbert, T. W. Kirchstetter, P. Berdahl, E. Bibian, L. S. Bruckman, D. Cremona, R. H. French, D. A. Gordon, et al., Soiling of building envelope surfaces and its effect on solar reflectance–part iii: Interlaboratory study of an accelerated aging method for roofing materials, Solar Energy Materials and Solar Cells 143 (2015) 581–590. doi:10.1016/j.solmat.2011.08.002.

[35] C. Ferrari, G. Santunione, A. Libbra, A. Muscio, E. Sgarbi, How accelerated biological aging can affect solar reflective polymeric based building materials, Journal of Physics: Conference Series 923 (2017) 012046. doi:10.1088/1742-6596/923/1/012046.

[36] R. Levinson, P. Berdahl, A. Berhe, H. Akbari, Effect of soiling and cleaning on reflectance and solar heat gain of a light-colored roofing membrane, Atmospheric Environment 39 (2005) 7807–7824. doi:10.1016/j.atmosenv.2005.08.037.

[37] M. LLC, Cool Roof Rating Council, `https://coolroofs.org/`, accessed: 2019-10-24.

[38] N. Alchapar, E. Correa, Aging of roof coatings. solar reflectance stability according to their morphological characteris-

tics, Construction and Building Materials 102 (2016) 297–305. doi:10.1016/j.conbuildmat.2015.11.005.

[39] E. Mastrapostoli, M. Santamouris, D. Kolokotsa, P. Vassilis, D. Venieri, K. Gompakis, On the ageing of cool roofs: Measure of the optical degradation, chemical and biological analysis and assessment of the energy impact, Energy and Buildings 114 (2016) 191 – 199. doi:doi.org/10.1016/j.enbuild.2015.05.030.

[40] C. Ferrari, A. Gholizadeh Touchaei, M. Sleiman, A. Libbra, A. Muscio, C. Siligardi, H. Akbari, Effect of aging processes on solar reflectivity of clay roof tiles, Advances in Building Energy Research 8 (1) (2014) 28–40. doi:10.1080/17512549.2014.890535.

[41] R. F. De Masi, S. Ruggiero, G. P. Vanoli, Acrylic white paint of industrial sector for cool roofing application: Experimental investigation of summer behavior and aging problem under Mediterranean climate, Solar Energy 169 (2018) 468–487. doi:10.1016/j.solener.2018.05.021.

[42] T. Aoyama, T. Sonoda, Y. Nakanishi, J. Tanabe, H. Takebayashi, Study on aging of solar reflectance of the self-cleaning high reflectance coating, Energy and Buildings 157 (2017) 92–100. doi:10.1016/j.enbuild.2017.02.021.

[43] X. Yang, C. Vang, D. Tallman, G. Bierwagen, S. Croll, S. Rohlik, Weathering degradation of polyurethane coating, Polymer Degradation and Stability 74 (2001) 341–351. doi:10.1016/S0141-3910(01)00166-5.

[44] B. Jelle, Accelerated climate ageing of building materials, components and structures in the laboratory, Journal of Materials Science 47 (2012) 6475–6496. doi:10.1007/s10853-012-6349-7.

[45] A. L. Pisello, E. Fortunati, C. Fabiani, S. Mattioli, F. Dominici, L. Torre, L. F. Cabeza, F. Cotana, Pcm for improving polyurethane-based cool roof membranes durability, Solar Energy Materials and Solar Cells 160 (2017) 34 – 42. doi:10.1016/j.solmat.2016.09.036.

[46] G. Santunione, C. Ferrari, C. Siligardi, A. Muscio, E. Sgarbi, Accelerated biological ageing of solar reflective and aesthetically relevant building materials, Advances in Building Energy Research (2018) 1–18doi:10.1080/17512549.2018.1488616.

[47] R. Ye, W. Lin, K. Yuan, X. Fang, Z. Zhang, Experimental and numerical investigations on the thermal performance of building plane containing CaCl2·6H2O/expanded graphite composite phase change material, Applied Energy 193 (2017) 325–335. doi:10.1016/j.apenergy.2017.02.049.

[48] C. Piselli, V. Castaldo, A. L. Pisello, How to enhance thermal energy storage effect of pcm in roofs with varying solar reflectance: Experimental and numerical assessment of a new roof system for passive cooling in different climate conditions, Solar Energy- doi:10.1016/j.solener.2018.06.047.

[49] R. Ricciu, L. A. Besalduch, A. Galatioto, G. Ciulla, Thermal characterization of insulating materials, Renewable and Sustainable Energy Reviews 82 (2016) 1765–1773. doi:10.1016/j.rser.2017.06.057.

[50] A. D'Alessandro, A. L. Pisello, C. Fabiani, F. Ubertini, L. F. Cabeza, F. Cotana, Multifunctional smart concretes with novel phase change materials: Mechanical and thermo-energy investigation, Applied Energy 212 (2018) 1448–1461. doi:10.1016/j.apenergy.2018.01.014.

[51] M. H. Chung, J. C. Park, Development of PCM cool roof system to control urban heat island considering temperate climatic conditions, Energy and Buildings 116 (2016) 341–348. doi:10.1016/j.enbuild.2015.12.056.

[52] A. L. Pisello, V. Castaldo, G. Pignatta, M. Santamouris, F. Cotana, Experimental in-lab and in-field analysis of waterproof membranes for cool roof application and urban heat island mitigation, Energy and Buildings 114 (2016) 180–190. doi:10.1016/j.enbuild.2015.05.026.

[53] ASTM D4329-13, Standard practice for fluorescent ultraviolet (uv) lamp apparatus exposure of plastics, Standard, ASTM International, West Conshohocken, PA (2013). doi:10.1520/D4329-13.

[54] ASTM G154-06, Standard Practice for Operating Fluorescent Light Apparathus for UV Exposure of Nonmetallic Materials, Standard, ASTM International, West Conshohocken, PA (2006). doi:10.1520/G0154-12A.

[55] ASTM E903-12, Standard Test Method for Solar Absorptance, Reflectance, and Transmittance of Materials Using Integrating Spheres, Standard, ASTM International, West Conshohocken, PA (2012). doi:10.1520/E0903-12.

[56] Angelantoni Test Technologies, http://www.acstestchambers.com/Product/Prodotto?id_fam= (2012).

[57] ASTM G173-03(2012), Standard tables for reference solar spectral irradiances: Direct normal and hemispherical on 37° tilted surface, Standard, ASTM International, West Conshohocken, PA (2012). doi:10.1520/G0173-03R12.

[58] A. V. Sá, M. Azenha, H. De Sousa, A. Samagaio, Thermal enhancement of plastering mortars with phase change materials: Experimental and numerical approach, Energy and Buildings 49 (2012) 1627. doi:10.1016/j.enbuild.2012.02.031.

[59] ISO 6946:2017, Building components and building elements – Thermal resistance and thermal transmittance – Calculation methods, Standard, International Organization for Standardization, Geneva, CH (2017). URL `https://www.iso.org/standard/40968.html`

[60] J. F. Kreider, P. S. Curtiss, A. Rabl, Heating and cooling of buildings: design for efficiency, edition, r Edition, Vol. 32, Taylor & Francis Group, 2013. doi:10.5860/choice.32-1554.

[61] V. Castaldo, V. Coccia, F. Cotana, G. Pignatta, A. L. Pisello, F. Rossi, Thermal-energy analysis of natural "cool" stone aggregates as passive cooling and global warming mitigation technique, Urban Climate 14. doi:10.1016/j.uclim.2015.05.006.